



JMWE (<https://www.jmwe.org>) is an open, peer-reviewed journal published under the CC BY-NC-SA 4.0 Creative Commons License. A version of this article was presented at the 2023 Sustainability in Ship Design and Operation conference at Webb Institute and US Merchant Marine Academy. Image adapted from Anton van den Wyngaerde, 1653.

A second look at the Propeller Sail high lift device for sailing cargo ships, using distributed, wing-mounted propellers

Sergio E. Perez, Lubomir A. Ribarov

U.S. Merchant Marine Academy, Department of Marine Engineering, Kings Point, NY
perezs@usmma.edu

Abstract:

The Propeller Sail, consisting of powered propellers mounted on ship wing-sails, is analyzed using computational fluid dynamics at Reynolds numbers up to 1 million. Lift and drag coefficients using two mounted propellers are calculated and compared with Flettner rotors. In addition, Propeller Sails with one contra-vortex propeller mounted on the sail wing tip are compared with one propeller mounted at mid-wing.

INTRODUCTION

In [1] the Propeller Sail concept was first introduced, consisting of ship wing-sails with powered propellers. This was a preliminary work using two-dimensional CFD (Computational Fluid Dynamics) simulations, which determined that the Propeller Sail may be a viable method for propelling ships, with lift coefficients as high as other high-lift devices such as Flettner rotors and suction sails. It was also found that tilting the propellers down by 20 degrees and placing the propellers on the trailing edge of the wing might produce higher lift with relatively low drag forces. Several possible usage methods were proposed: Propeller Sails mounted at the bow and stern of a ship to function as thrusters, and using Propeller Sails in lieu of propellers in the water, which may reduce construction costs and increase hull efficiency. Also considered was that induced drag might be lowered by the use of contra-vortex propellers (spinning against wingtip vortices) at sail wingtips. A one-propeller Propeller Sail test model is presented in Figure 1.



Figure 1. The Propeller Sail model with one propeller.

In this work, 3-Dimensional CFD simulations were conducted with a NACA 0030 wing section mounted on a smooth and unobstructed deck. Simulations were made without propellers, with one propeller alone operating at the wingtip, with one propeller alone operating at mid-wing, and with two propellers operating concurrently. Only 30-degree wing angles of attack were tested in this work, with the propeller rotation axes at ten degrees below the angle of the wings, at a variety of propeller rotational speeds. No attempts were made to optimize the design of the propellers or their angle or position relative to the wing.

Limited model tests were conducted with the 1m model displayed in Figure 1.

CFD SIMULATIONS

SimScale [2], a RANS (Reynold Averaged Navier-Stokes) CFD (Computational Fluid Dynamics) product, was used for the 3-dimensional CFD simulations. SimScale accesses the well-tested OpenFOAM CFD platform [3], and provides cloud-based parallel processing.

The simulated wing uses a NACA 0030 profile, with 6.9 m height and 2.29 m chord. The mesh is composed of 13.3 M cells, and is divided into four regions of mesh size refinement, as partially shown in Figure 2. The regions include the surface of the propellers, the area near the propeller, a near-field region and a far-field region. Overall mesh quality is calculated by the SimScale software as 0.499688 (the acceptable range is from 0.035 to 1.0), and is based on non-orthogonality of the cells (please see Appendix 1 for a mesh-quality summary). Simulation runs typically used about 100 “core-hours” while running in parallel mode for about 1-2 hours of real-time.

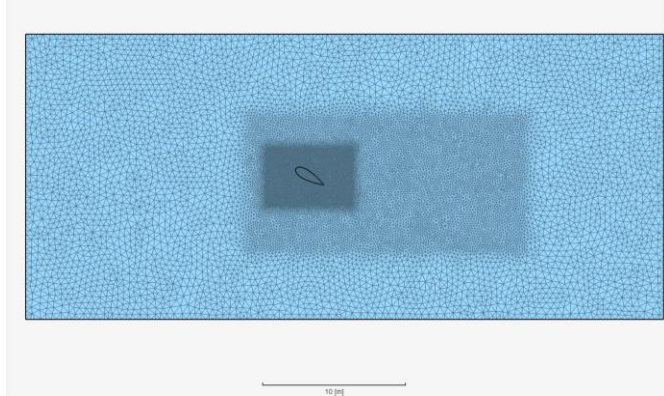


Figure 2. The simulation domain and mesh refinement regions. The wing-sail is seen from above.

Modeling the rotation of the propellers in SimScale is simplified by the use of a Modified or Moving Reference Frame (MRF) around the propellers, in which the propellers are static, but rotating flow is imposed around them in the MRF.

A mesh refinement study was conducted, with total cell counts ranging from 5 to 13.1 million cells. The mesh size was varied in all of the refinement regions, but not always in a uniform way: if the propeller faces had a finer mesh, the near field and far field might be made slightly coarser. Figure 3 shows the wing lift and drag results used for the mesh refinement study. Two propellers in simultaneous operation on the wing were modeled, turning at 100 rad/s, with 10 m/s winds.

It appears that the difference between the results from mesh sizes greater than 5M are fairly small. The 13.1M cell-mesh was used for this study.

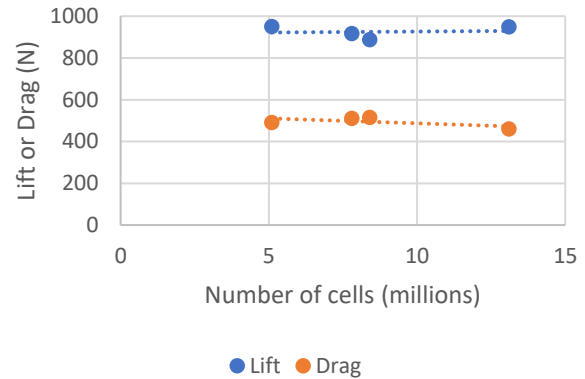


Figure 3. Mesh refinement study results.

We can also say in general terms that similar CFD simulations using far less than the 13.1 million cells used in this study have produced acceptable results. For example, in [4] a drone propeller was modeled with Thrust and Pressure coefficients within 8% of experimental values, using 1 million cells. Initial calculations performed for this work showed that using the automatic physics-based meshing tool of SimScale with 3.1 million cells on a NACA 2424 wing (closely resembling the NACA 0030 used here) gave lift coefficients that were within 6% and drag coefficients 16%-29% of experimental values.

The propellers were “stock” 3D files downloaded from an open-source 3-D geometry library [5], and placed on the aft end of the wing. As will be seen in the Results section, the propeller efficiency was quite low.

The motors driving the propellers were assumed to be inside the wing, but the shafts connecting the wing and propeller were not modeled. The propeller axes of rotation were tilted downwards ten degrees from the wings, and the wings were set to an angle of attack of 30 degrees into the incoming flow. Propeller diameter was 1.42 m. No attempt was made to optimize the propeller design, size, angle or placement on the wing. Figure 4 shows the Propeller Sail as modeled.

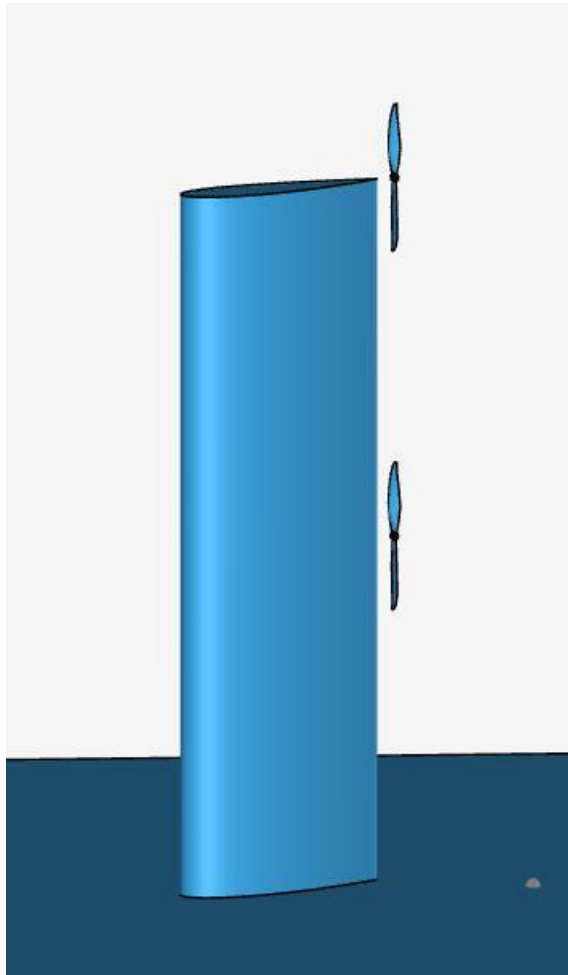


Figure 4. The wing and propeller configuration.

Figure 5 shows the computational domain, with air flow entering from the left side (4 faces have been hidden for clarity). Boundary conditions were set to “Pressure” at the exit, “No-slip” at the bottom and “Pressure inlet-outlet” at the sides and top of the virtual tunnel.

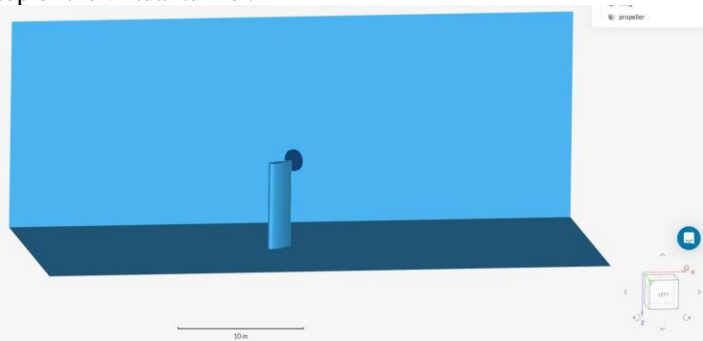


Figure 5. Virtual wind tunnel. Only one propeller zone is visible. The disc seen at the wingtip is the MRF zone which encloses the propeller.

SimScale was run at wind speeds of 4 and 10 m/s, and rotational speeds of 50, 100, 200 and 400 radians/s. The program output provided lift and drag forces as well as moments on the wing and propellers.

A second look at the Propeller Sail high lift device for sailing cargo ships, using distributed, wing-mounted propellers.

RESULTS

One propeller only: Wingtip mounted vs mid-mounted

A possible use of the Propeller Sail involves only one propeller on the wing. The question arises: is there an advantage to mounting the propeller at the wingtip as compared to a point closer inboard? CFD runs were made at propeller speeds of 200 rad/s with a relative wind of 10 m/s (the relative wind is the vector sum of the wind and vessel velocities), with the propeller on two positions: on the wingtip and “mid-wing” (2 meters below the wingtip, as shown in Figure 4). The propellers were turning in a contra-vortex direction.

The results are presented on Figure 6. At the conditions tested, the mid-wing configuration generates about 50% more lift, with a 50% higher Lift/Drag ratio than the wingtip mounted configuration.

On figure 6, Wing Lift and Wing Drag represent the force experienced by the wing alone as the propeller turns. We note that the propeller thrust has a component in the opposite direction as the wing drag, and hence has a negative sign. The total lift and total drag represent the sum of wing and propeller forces – the thrust from the propeller has a component that minimizes total wing drag and increases wing lift.

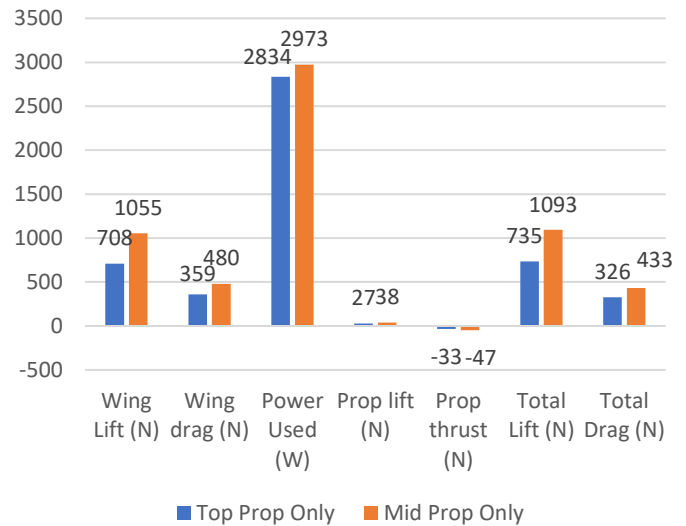


Figure 6. Lift, drag and power for Propeller Sails with wingtip mounting vs mid-wing mounting, at 10 m/s, 200 radians/s, and 30 degree angle of attack.

It appears that, if only one propeller is to be used, the mid-wing configuration is the better choice under the limited conditions tested. In [1], it was postulated that the contra-vortex rotation of wingtip mounted propellers could minimize drag, as discussed in [6] and [7], but the results in the current work show that, while the drag force on the wingtip mounted configuration is

lower, the lift force is substantially lower. As tested, there does not appear to be an advantage to using a wingtip mounted propeller vs a mid-wing mounted propeller.

Two-propeller results

Effect of propeller power

CFD runs were conducted on the 2-propeller configuration shown in Figure 4. Figure 7 below shows Total lift and drag on the Propeller Sail as a function of total power into the propellers, with a relative wind of 10 m/s. One can see that, at low power (less than about 2 kW), a small increase in power results in a relatively large increase in lift and drag. At power values greater than about 2 kW, there is a transition in behavior where drag and lift are much less sensitive to power. In addition, drag decreases after the transition point due to the increasing thrust of the propellers.

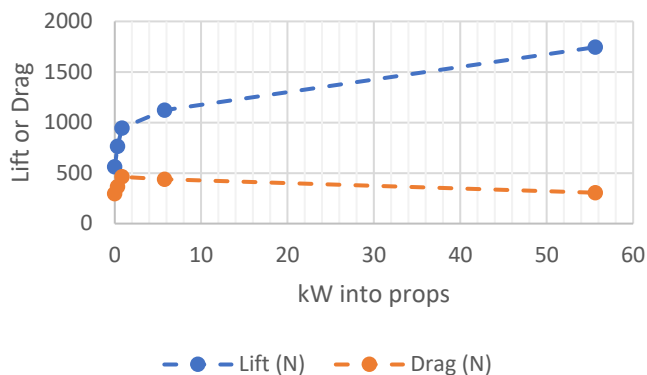


Figure 7. Total lift and drag on the wing (including contributions from 2 propellers), with relative wind speed of 10 m/s.

The change in behavior after the transition may be attributable to the elimination of flow separation on the suction side (top) of the wing. CFD images in Figure 8 show separating flow at 0.3 kW and 50 rad/s, which is well below the transition point occurring at about 2 kW. The figure also shows very little separation at 200 rad/s and 5.7 kW, supporting this hypothesis.

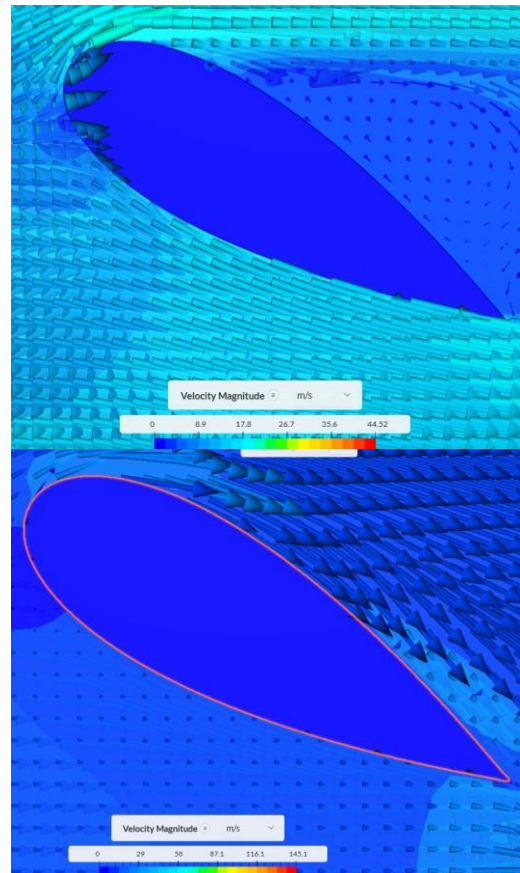


Figure 8. At top, separation at low propeller power of 237 W, and at bottom, separation is greatly diminished at 5.7 kW.

We may then propose that, below the transition point, any increase in lift is due to a combination of reduced separation and increased flow speed over the airfoil, resulting in a greater rate of change in lift than after the transition point, when lift increases are due to increased flow speed only.

It appears that lift and drag will continue to increase to very high numbers as long as sufficient power is provided.

Effect of incoming flow speed

As might be expected, the faster the relative wind entering the Propeller Sail, the greater the lift and drag forces. Figure 9 shows that when the propeller is activated there is a proportionately higher increase in lift and drag at low relative wind speeds: at a relative wind speed of 4 m/s, lift increases from 89 to 207 at 1.04 kW (increase in lift by a factor of 2.32 times), while at 10 m/s lift increases from 562 to 945 N (increase in lift by a factor of 1.68 times).

Figure 9 also shows that the lower the wind speed, the less power is required to achieve zero drag.

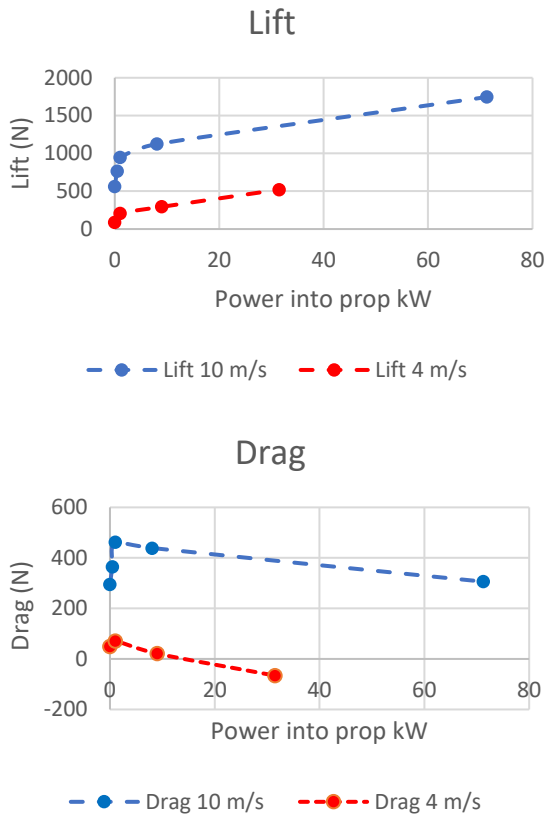


Figure 9 Effect of relative wind on lift and drag of Propeller Sail

Lift and Drag Coefficients

The normal expressions for lift and drag ($Lift = 0.5\rho V^2 A C_l$ and $Drag = 0.5\rho V^2 A C_d$, where C_l and C_d are lift and drag coefficients) must be used with care with Propeller Sails, as C_l and C_d also depend on relative wind speed, propeller size, design, power input, tilt angle, number and arrangement. But C_l and C_d can be useful for comparing very specific Propeller Sail designs with other lift-producing methods at the same wind speed, size and power.

Consider the C_l and C_d plots for two identical Propeller Sails, but exposed to different relative wind speeds, as shown in Figure 10. The blue lines represent C_l , and the red lines C_d . Solid lines are at 10 m/s and dashed lines at 4 m/s. Clearly, despite the Propeller Sails being identical, the lift and drag coefficients at one relative wind speed can be quite different from lift and drag coefficients at another wind speed.

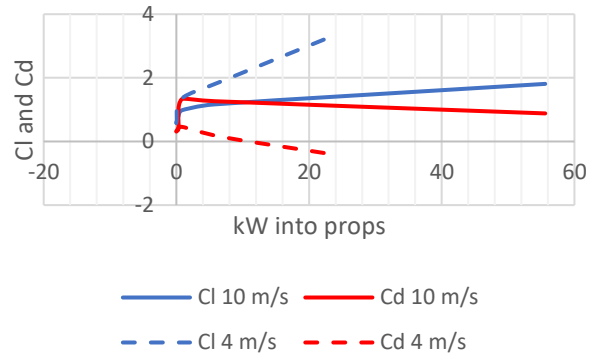


Figure 10. The effect of wind speed and power on C_l and C_d .

We note that turning on the propeller power to about 24 kW caused an increase in C_l by a factor of almost 6 times, for 4 m/s wind speed, from 0.46 to 3.4. At about 0.7 kW, the lift coefficient increased by a factor of about 3 times, from 0.46 to 1.34. The rather low non-powered wing lift coefficient of 0.46 is due to the 30 degree angle of attack of the wing.

Propeller Performance Characteristics

SimScale CFD software gives moments (M_x , M_y and M_z) and forces (F_x , F_y and F_z) on the propellers in the x, y and z axes. These were used to calculate propeller parameters:

$$Thrust = (F_x^2 + F_y^2 + F_z^2)^{1/2} \quad (1)$$

$$Torque = (M_x^2 + M_y^2 + M_z^2)^{1/2} \quad (2)$$

$$Thrust Coefficient \quad C_t = \frac{Thrust}{\rho D^4 n^2} \quad (3)$$

$$Torque Coefficient \quad C_q = \frac{Torque}{\rho D^5 n^2} \quad (4)$$

$$Power Coefficient \quad C_p = 2 \pi C_q \quad (5)$$

$$Advance Ratio \quad J = \frac{V}{n D} \quad (6)$$

$$Efficiency = \frac{C_t J}{C_p} \quad (7)$$

$$Power = Torque \times \text{nrad} \quad (8)$$

In the equations above, ρ is air density = 1.22 kg/m³, D is the propeller diameter, n is the propeller revolutions/s and nrad is propeller radians/s.

Figure 11 below shows the very low efficiency of the propeller mounted at mid-wing, as a function of advance ratio J . As mentioned earlier, the propeller was a “stock” open-source model from a 3D model website [4] which was not optimized in any way. Real propellers can have efficiencies of about 0.8 and greater, and have efficiency plots of similar form to Figure 11 [7].

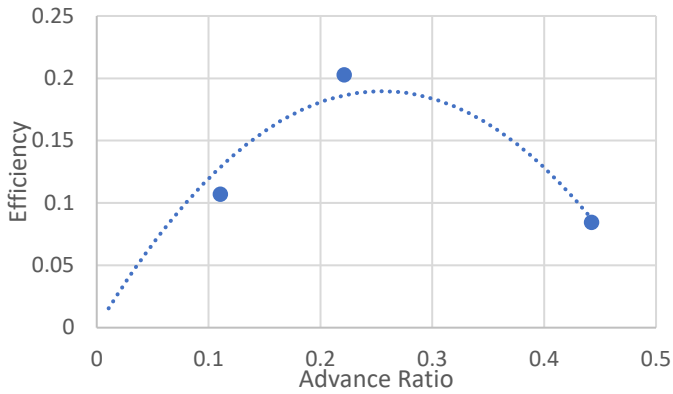


Figure 11. Mid-Wing propeller efficiency at 10 m/s relative wind velocity.

Comparison with Flettner rotors

The authors of [8] give lift, drag and power data for Flettner rotors with infinite aspect ratios at Reynolds numbers of $1.8E5$ to $1E6$. Data from [8] were used to produce Figure 12, which shows C_l and C_d as a function of spin ratio ($V_{\text{tangential rotor}}/V_{\text{wind}}$), as well as Figure 13 showing Power coefficient $P_w = \frac{\text{Power}}{\frac{1}{2}\rho V^3 \text{Area}}$.

The area is the product of Flettner rotor's height and diameter. The Flettner rotor and Propeller Sail were compared at the same wind velocity (4 m/s) and dimensions (6.9 m x 2.29 m), but not at the same aspect ratio. The effective aspect ratio (wingspan x 2 / chord) of the Propeller Sail wing is 6, while that of the Flettner rotor from [8] is infinite (the rotor extended to the top of the wind tunnel test section). In [9], the authors tested Flettner rotors at a variety of aspect ratios. It appears that, at the Flettner rotor spin ratio of 1.8 used here, the effect of aspect ratio on the lift forces from 6 to 8 is relatively small, indicating that the difference in C_l between $AR = 6$ and $AR = \infty$ might give an advantage to the Flettner rotor on the order of about 10%.

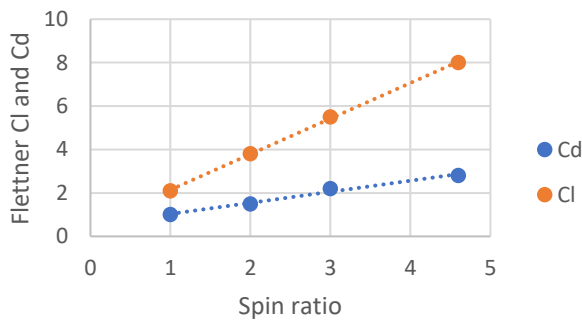


Figure 12. C_l and C_d results (for Flettner rotor) as a function of the spin ratio $V_{\text{tangential}}/V_{\text{freestream}}$.

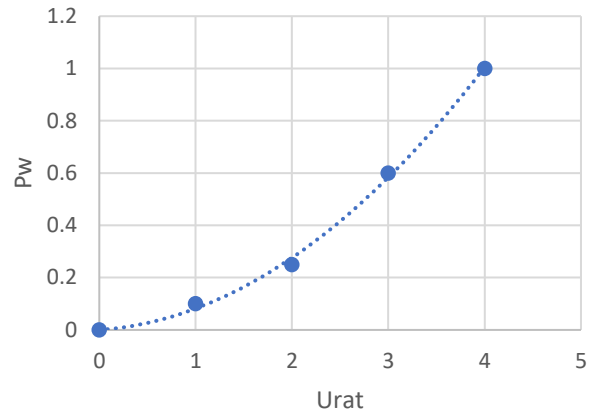


Figure 13. Flettner rotor Power Coefficient P_w as a function of spin ratio.

Figure 14 below shows that the Propeller Sail requires about 4 times the power as the Flettner rotor to produce the same lift coefficient of 3.4 at 4 m/s wind speed.

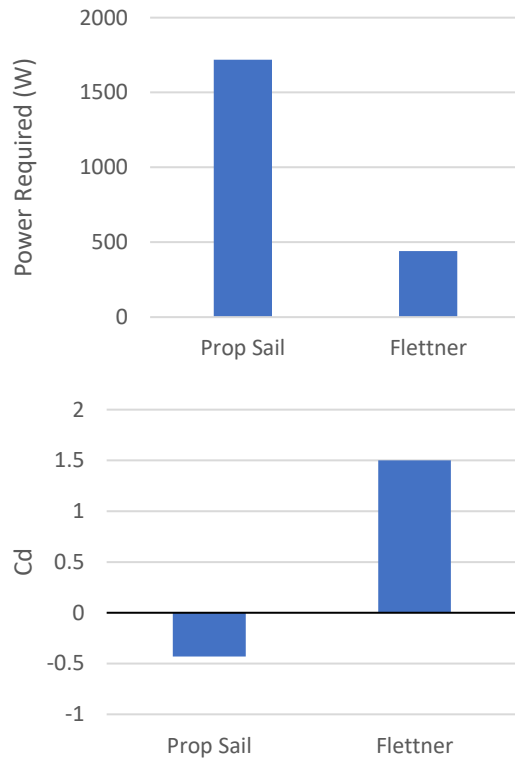


Figure 14. Top: Power required (Watts) for $C_l = 3.4$ in 4 m/s winds. Bottom: Drag coefficient C_d at C_l of 3.4.

Since the efficiency of the propeller is so poor, in Figure 14 the "Power required" for the Propeller Sail has been multiplied by the calculated efficiency 0.0570 and divided by 0.8, to represent a more reasonable estimate of power to turn the propellers. The drag coefficient shown on Figure 14 gives reason for optimism: the Propeller Sail has a negative drag coefficient, indicating that downwind drift is being resisted by the propeller thrust, while the Flettner rotor gets pushed downwind. The

A second look at the Propeller Sail high lift device for sailing cargo ships, using distributed, wing-mounted propellers.

upwind force created by the Propeller Sail can be traded for greater lift by pointing the propeller further upwind.

Model Testing Results

A ship model was assembled using a discarded 1m balsa hull with similar lines to a Series 60 C2 ship, a multi-engine model airplane wing, electric motor/propeller, battery, and radio control equipment, seen in Figure 15 before and after finishing. Since to the best of our knowledge a ship like this had never been built, the goal of the tests was modest: to determine if there were any obvious impediments to using the Propeller Sail concept to move a ship.

The propeller spin rate and rudder could be controlled remotely, but the angle of the sail relative to the ship model was set before each run. The propeller spun in a contra-vortex direction.



Figure 15. Ship Model before- and after full assembly. Lower figure shows remote controlled rudder and propeller. The aileron was not used in tests.

The ship model was ballasted to bring the water level to the fully-laden design water line. Tests determined that:

- The ship model can stably move in any direction into the wind when power is applied.
- Rudder control is quite effective as long as speed is not too low.

A second look at the Propeller Sail high lift device for sailing cargo ships, using distributed, wing-mounted propellers.

- The ship model sailed quite well with and without the propeller activated.
- When the ship model was in pure sailing mode, an increase in speed was evident when the engines were activated even at relatively low propeller RPM's.
- Application of maximum power in directions away from the longitudinal produced a noticeable (but not de-stabilizing) list. This was at power levels far higher than what might normally be used.

Videos of the model may be seen at:

- Downwind run with low power on <https://youtu.be/ofmo3aF10nc>
- Moving directly into wind at low power, followed by downwind turn: <https://youtu.be/D13Rzl8eIHI>
- List when high power is applied while sailing downwind: <https://youtube.com/shorts/bO34H8ISBo>
- Two laps in light winds using two levels of power: <https://youtu.be/MuRGIXDHTFU>

CONCLUSIONS

In limited CFD trials, the Propeller Sail required about 4 times the power of a Flettner rotor when producing a lift coefficient of 3.4, in 4 m/s winds and a Reynolds number of 1 million. It is important to note that, during the same test, the Propeller Sail achieved a drag coefficient -0.43, as compared to +1.5 for the Flettner. The Propeller Sail negative lift coefficient is a result of the propeller creating an upwind force that could mitigate or eliminate the downwind drift of a vessel. This could be a very useful feature, especially on vessels with small or nonexistent keels or appendages designed to minimize downwind drift.

Testing of the Propeller Sail on a remotely controlled model cargo ship showed that there appear to be no obvious impediments to the use of the concept, as the model worked well with and without the propeller activated.

The Propeller Sail is a concept still in its infancy, and requires much further study to determine its viability for wind-assisted shipping. This will include parametric CFD testing of propeller and airfoil design, size and positions, as well as the use of wingtip fences as in [6] and [7].

To be considered in any viability analysis are the fuel savings the Propeller Sail might afford when used in pure sailing mode, the maneuvering benefits of bow and stern Propeller Sails, as well as the reduction in hull drag and ship construction costs that using only wing-mounted engines might provide (that is, no conventional propeller under the water surface).

REFERENCES

- [1] Preliminary Analysis of a new high lift device for sailing cargo ships using distributed wing-mounted propellers, S.E. Perez, Journal of Merchant Ship Wind Energy, February 2023, <https://www.jmwe.org>
- [2] SimScale, <https://www.simscale.com>
- [3] OpenFOAM, <https://www.openfoam.com>
- [4] Validation Case: Drone Propeller Study, <https://www.simscale.com/docs/validation-cases/drone-propeller-study/>
- [5] GrabCAD, <https://grabcad.com>
- [6] Effects of wingtip-mounted propeller on wing lift, induced drag and shed vortex pattern; M. Snyder, Ph.D. thesis, Oklahoma State University, May, 1967
- [7] Wingtip-mounted propellers: aerodynamic analysis of interaction effects and comparison with conventional layout; Tomas Sinnige, Tom Stokkermans, Nando van Arnhem, Georg Eitelberg, Journal of Aircraft, November 2018
- [8] Experiments on a Flettner rotor at critical and supercritical Reynolds numbers G. Bordogna, S. Muggiasca, S. Giappino, M. Belloli, J.A. Keuning, R.H.M. Huijsmans, A.P. van 't Veer, Journal of Wind Engineering and Industrial Aerodynamics, 188 (2019) 19-89 <https://doi.org/10.1016/j.jweia.2019.02.006>
- [9] Flettner Rotor Concept for Marine Applications: A Systematic Study, A. De Marco, S. Mancini, C. Pensa, G. Calise, and F. De Luca, International Journal of Rotating Machinery Volume 2016, <http://dx.doi.org/10.1155/2016/3458750>

APPENDIX

Mesh Analysis

SimScale incorporates Simulation Modeling Suite(TM) software by Simmetrix Inc. © 1997-2023. All Rights Reserved.

Model import took 4.631900971s.

Maximum precision of model and its entities: 2.7244077608409207e-05 m.

Absolute small feature tolerance: 0.00024578644961199104 m.

Surface meshing took 3m35.820114222s.

Number of cells after 5m23.748154465s: 319692

Number of cells after 7m11.640438659s: 9124597

Number of cells after 8m59.550717453s: 11935179

The mesh may be finer than desired. Please check the model and the mesh settings

Number of cells after 10m47.497306174s: 11576363

Number of cells after 12m35.421802035s: 13202029

Number of cells after 14m23.312525853s: 14528030

Number of cells after 16m11.190953464s: 13264977

Number of cells after 17m59.110667262s: 13263074

Meshing took 19m19.357746208s. Starting mesh export.

Mesh quality metrics:

tetEdgeRatio

Acceptable range: 0 to 100

min: 1.0000000000000009

max: 20.078545752398234

average: 1.6921194980580068

standard deviation 0.2602519165882951

median: 1.6854332552083646

99.9-th percentile: 2.669404959272894

99.99-th percentile: 7.2847162902410245

99.999-th percentile: 11.210901206392863

quadMaxAngle

Acceptable range: 90 to 200

min: 89.50855908783534

max: 206.13586363715666

average: 90.17323720538215

standard deviation 2.1971038468751374

median: 90

99.9-th percentile: 128.47631900015136

99.99-th percentile: 156.08465130182734

99.999-th percentile: 175.11571470369145

triMaxAngle

Acceptable range: 60 to 160

min: 59.99999999999999

max: 173.99358257911967

average: 80.18341966910695

standard deviation 13.015130217014363

median: 76.41192526400934

99.9-th percentile: 116.28758499376791

99.99-th percentile: 121.17655982777752

99.999-th percentile: 149.61837238383612

triMinAngle

Acceptable range: 10 to 60

min: 0.5371069397580727

max: 59.99999999999999

average: 45.524047713582036

standard deviation 8.143350895974113

median: 45.669640235991395
99.9-th percentile: 59.82928251372292
99.99-th percentile: 59.997502165788084
99.999-th percentile: 59.99999999999981

volumeRatio

Acceptable range: 0 to 100

min: 1
max: 87.3536778989241
average: 1.3632926491074917
standard deviation 0.7968357594104875
median: 1.0512707083559942
99.9-th percentile: 7.053507257018633
99.99-th percentile: 9.60712082095733
99.999-th percentile: 13.794221463145591

tetAspectRatio

Acceptable range: 0 to 100

min: 1.0000000000000002
max: 53.91536355889224
average: 1.6095270884877317
standard deviation 0.2766145970946696
median: 1.6633940211680334
99.9-th percentile: 2.106229247915763
99.99-th percentile: 4.200279861948586
99.999-th percentile: 25.871779099251683

nonOrthogonality

Acceptable range: 0 to 88

min: 0
max: 86.91916232092346
average: 10.824626218050406
standard deviation 12.19770195592239
median: 4.9561633679237564
99.9-th percentile: 45.45996750540194
99.99-th percentile: 60.02186167456459
99.999-th percentile: 80.33881125254182

skewness

Acceptable range: 0 to 100

min: 0
max: 8.645174696551125
average: 0.13209216397957685
standard deviation 0.14867386375044425
median: 0.11254597059168074
99.9-th percentile: 0.9231817368773678
99.99-th percentile: 1.1970368479630886
99.999-th percentile: 2.8306147992653905

aspectRatio

Acceptable range: 0 to 100

min: 1
max: 53.91536355889224
average: 1.4107955557857645
standard deviation 0.3649810885803656
median: 1.424802277222787
99.9-th percentile: 2.0714943826284173
99.99-th percentile: 3.5322265820576497
99.999-th percentile: 23.719382459145773

Overall mesh quality (based on the 99.99-percentile): 0.499688

Acceptable range: 0.035 to 1.0

Overall mesh quality is computed from:

Non Orthogonality: 60.020658 (normalized value: 0.499688, weight: 1.00)